Published in final edited form as:
Cell Metab. 2015 January 6; 21(1): 51–64. doi:10.1016/j.cmet.2014.12.002.

Peroxisomal lipid synthesis regulates inflammation by sustaining neutrophil membrane phospholipid composition and viability

Irfan J. Lodhi[1], **Xiaochao Wei**[1], **Li Yin**[1], **Chu Feng**[1], **Sangeeta Adak**[1], **Grazia Abou-Ezzi**[2], **Fong-Fu Hsu**[1], **Daniel C. Link**[2], and **Clay F. Semenkovich**[1,3]

[1]Division of Endocrinology, Metabolism & Lipid Research, Washington University School of Medicine, St. Louis, MO 63110, USA

[2]Oncology Division, Department of Medicine, Washington University School of Medicine, St. Louis, MO 63110, USA

[3]Department of Cell Biology & Physiology, Washington University School of Medicine, St. Louis, MO 63110, USA

SUMMARY

Fatty acid synthase (FAS) is altered in metabolic disorders and cancer. Conventional FAS null mice die in utero so effects of whole body inhibition of lipogenesis following development are unknown. Inducible global knockout of FAS (iFASKO) in mice was lethal due to a disrupted intestinal barrier and leukopenia. Conditional loss of FAS was associated with the selective suppression of granulopoiesis without disrupting granulocytic differentiation. Transplantation of iFASKO bone marrow into wild type mice followed by Cre induction resulted in selective neutrophil depletion but not death. Impaired lipogenesis increased ER stress and apoptosis in neutrophils by preferentially decreasing peroxisome-derived membrane phospholipids containing ether bonds. Inducible global knockout of PexRAP, a peroxisomal enzyme required for ether lipid synthesis, also produced neutropenia. FAS knockdown in neutrophil-like HL-60 cells caused cell loss that was partially rescued by ether lipids. Inhibiting ether lipid synthesis selectively constrains neutrophil development, revealing an unrecognized pathway in immunometabolism.

Correspondence: csemenko@wustl.edu.

AUTHOR CONTRIBUTIONS

I.J.L. conceived the hypothesis, designed and conducted experiments, and wrote the manuscript. X.W. conducted experiments and edited the manuscript. L.Y., C.F., S.A., and G.A.-E. conducted experiments and interpreted data. F.-F.H. performed mass spec analyses, assigned structures of lipid molecules, and interpreted data. D.C.L. designed experiments related to granulopoiesis, and wrote the manuscript. C.F.S. secured funding and regulatory approvals, coordinated collaborations, designed experiments, and wrote the manuscript.

INTRODUCTION

De novo lipogenesis, the endogenous production of fats from simple precursors, is altered in multiple diseases, including obesity, diabetes and cancer (Menendez and Lupu, 2007; Moreno-Navarrete et al., 2009; Roberts et al., 2009). The multifunctional enzyme fatty acid synthase (FAS) catalyzes the first committed step in *de novo* lipogenesis. After priming with acetyl-CoA, FAS uses malonyl-CoA as a 2-carbon source and NADPH as a cofactor to synthesize palmitate, a 16-carbon saturated fatty acid. Mammalian FAS contains all of the necessary enzymatic activities in a single polypeptide to convert malonyl-CoA to palmitate. Although liver and adipose tissue are the two main sites of FAS-mediated lipogenesis, FAS is ubiquitously expressed and regulated at transcriptional as well as post-transcriptional levels. Insulin and glucose promote FAS expression through the transcription factors SREBP1 and ChREBPα, respectively (Jensen-Urstad and Semenkovich, 2012). FAS is also regulated by phosphorylation of distinct subcellular pools of the protein (Jensen-Urstad et al., 2013).

A series of tissue-specific conditional knockout models of FAS implicate this enzyme in integrative physiology. A common theme in these studies is that FAS may channel newly synthesized palmitate to specific subcellular compartments to transmit signals relevant to metabolic disorders. In liver, brain and macrophages, FAS appears to be required for endogenous activation of the nuclear receptor PPARα (Chakravarthy et al., 2009; Chakravarthy et al., 2005; Chakravarthy et al., 2007; Schneider et al., 2010), a transcriptional regulator of fatty acid oxidation and gluconeogenesis (Reddy and Hashimoto, 2001). In the endothelium and intestinal epithelium, FAS provides substrate for palmitoylation of key proteins to maintain tissue integrity (Wei et al., 2011; Wei et al., 2012). In cardiac and skeletal muscle, FAS is required for calcium flux (Funai et al., 2013; Razani et al., 2011). In neural tissues, FAS is important for stem cell renewal (Knobloch et al., 2013). In adipose tissue, FAS may be involved in the endogenous activation of PPARγ, a nuclear receptor critical for adipose tissue development and function. Mice with adipose specific deletion of FAS resist diet-induced obesity and glucose intolerance, and have increased energy expenditure with browning of subcutaneous white adipose tissue (Lodhi et al., 2012).

Given the diverse tissue-specific effects of FAS, it is difficult to predict aggregate effects of whole body FAS inhibition in an adult, information relevant to pharmacologic strategies aimed at inhibiting lipogenesis. The FAS null mutation induces embryonic lethality (Chirala et al., 2003), so mice with conventional FAS deficiency have not been available. Here we describe inducible global FAS knockout in adult mice. Unexpectedly, these mice die from neutropenic sepsis soon after the knockout. Neutropenia appears to result from increased programmed cell death caused by impaired lipogenesis, which disrupted membrane phospholipid composition, especially ether lipid content. We also generated mice with inducible deficiency of ether lipid synthesis and found neutropenia in the setting of decreased membrane ether lipid content. These findings uncover a novel relationship between lipogenesis and inflammation, and establish a model for selective inactivation of the neutrophil lineage.

RESULTS

Tamoxifen-inducible Global Deletion of FAS in Adult mice is Lethal

To avoid the embryonic lethality of the FAS null mutation, we generated tamoxifen-inducible FAS knockout (iFASKO) mice by crossing mice $FAS^{lox/lox}$ mice with Rosa26-CreER mice, transgenic mice expressing Cre recombinase fused to the estrogen receptor ligand binding domain (CreER) under the control of the ubiquitously expressed Rosa26 promoter (Figure S1A) (Badea et al., 2003). Control (floxed without Cre) and iFASKO mice were treated daily with tamoxifen (50 μg/g body weight) for 5 consecutive days. FAS mRNA was decreased in multiple tissues of tamoxifen-treated iFASKO mice, including liver, kidney and white adipose tissue, but not in the hypothalamus (Figure S1B). Western blot analysis confirmed that there was no knockout in the hypothalamus or whole brain (Figure S1C), suggesting that phenotypes are not likely due to direct CNS effects.

Following tamoxifen treatment, iFASKO mice abruptly lost weight. By day 7, body weight was 30% lower (Figure 1A) in the setting of a dramatic decrease in food and water intake (Figures 1B and C). Control mice manifested transient effects on appetite with tamoxifen as often seen with this agent, but resumed normal food intake after treatment (Figure 1B). All iFASKO mice died within 10 days of the initial tamoxifen dose (Figure 1D). To determine if dietary lipids could compensate for the lack of endogenously synthesized lipids, we fed a high fat diet to control and iFASKO mice for four weeks then administered tamoxifen while continuing the high fat diet. This dietary intervention did not rescue iFASKO mice (Figure 1E), suggesting that endogenously produced lipids have effects that cannot be replaced by dietary lipids.

Gonadal white adipose tissue (WAT) depots in the mutant mice were strikingly decreased compared to control mice (Figure 1F). MRI-determined body composition on day 7 after tamoxifen treatment showed decreased adiposity and leanness in the iFASKO mice treated with tamoxifen (Figure 1G).

PPARα is a ligand-activated nuclear receptor enriched in liver where it is important for fatty acid oxidation, ketogenesis, lipid transport and gluconeogenesis (Bernal-Mizrachi et al., 2003). Consistent with previous studies suggesting that liver FAS regulates endogenous activation of PPARα (Chakravarthy et al., 2005), hepatic PPARα-dependent gene expression was decreased in iFASKO mice, and mice had hepatic steatosis (Figure S2A-C). Serum chemistries are presented in Figure S2D-G. Neither conditional FAS deficiency in liver nor whole body PPARα deficiency is associated with lethality.

Compromise of the Intestinal Barrier in iFASKOS Mice

Necropsies of iFASKO mice showed no gross lesions in the lung, heart, brain, thymus, lymph nodes, adrenal, pituitary, middle ear, or eye. However, epithelial cells in the colon were disordered at the luminal border, suggesting compromise of the intestinal barrier (Figure 2A).

Restricting bacteria to the intestinal lumen maintains the mutually beneficial relationship between mammalian host and the intestinal microbiota (Hooper, 2009). A mucus barrier that

overlies the intestinal epithelium and is derived from goblet cells provides this anatomical restriction. The large gel-forming protein Mucin 2 (Muc2), a key component of mucus (Johansson et al., 2009), requires FAS-mediated *de novo* lipogenesis for its palmitoylation and secretion. Mice with FAS inactivation specifically in epithelial cells of the colon have a severe disruption of the intestinal mucus barrier, increased intestinal permeability and systemic inflammation, resulting in reduced viability (Wei et al., 2012). Alcian blue staining of goblet cells and mucin revealed disruption of the mucus layer in iFASKO mice (Figure 2B). Serum levels of bacterial endotoxin and the inflammatory cytokine TNFα were elevated in the knockout mice (Figure 2C-D). These results suggest that impaired intestinal barrier function allows access of the intestinal microbiota to the circulation leading to septicemia and death in iFASKO mice following Cre induction, confirming our findings in mice with intestine-specific FAS inactivation (Wei et al., 2012). Given the pleiotropic physiological roles of FAS, it is also possible that other epithelial barriers may be compromised with loss of FAS. As noted above, there were no gross lesions in the lungs of these mice. Histopathologic examination of lungs from necropsies showed no evidence of pneumonitis and identified no significant lesions. A few lung arterioles appeared to contain increased platelets, but these small foci lacked the structure to allow identification as thromboemboli. Representative photomicrographs from lung are presented in Figure S2H.

A minority of intestine-specific FAS deficient mice dies as compared to the complete lethality in iFASKO mice, suggesting involvement of an additional pathogenic mechanism.

FAS Knockout Disrupts Myelopoiesis

Despite abnormal intestinal architecture and systemic endotoxemia, surprisingly there was no cellular inflammatory infiltrate in the gut (Figure 2). Inflammatory cells were also sparse upon histologic examination of blood vessels supplying multiple organs such as the liver and kidney (not shown). The lack of tissue neutrophils in tissues of septic mice suggested a potential defect in the machinery of the inflammatory response such as leukocytes. Blood counts revealed ~70% fewer white blood cells in peripheral blood of iFASKO mice due primarily to the absence of neutrophils (Figure 3A). Decreased T cells and a trend to decreased monocytes were also observed. Red blood cell counts were unaffected, but platelets were increased in the mutant mice (Figure 3B).

Bone marrow is the primary site of granulopoiesis and serves as a reservoir for mature neutrophils (Day and Link, 2012). The bone marrow in iFASKO mice 7 days after the first injection of tamoxifen (just prior to death) was hypocellular (Figure 3C). The spleen is a major site of extramedullary hematopoiesis in the setting of bone marrow failure. However, the spleen was smaller and appeared necrotic in iFASKO mice (Figure 3D). Interestingly, the serum level of granulocyte colony stimulating factor (G-CSF), the principal cytokine regulating granulopoiesis that is often induced in response to neutropenia (Liu et al., 1996), was dramatically elevated in iFASKO mice (Figure 3E).

To address potential mechanisms underlying the bone marrow phenotype, we treated mice with tamoxifen for 3 days followed by analyses on day 4, a shorter course than the 5 days associated with complete loss of neutrophils, to allow us to study neutrophils prior to their ablation. With this approach, gene expression in marrow was notable for decreased FAS

mRNA but there was no effect on the message for lymphoid enhancer-binding factor 1 (LEF-1) (Figure S3), a transcription factor critical for proliferation, survival and differentiation of granulocyte progenitor cells (Skokowa et al., 2006; Skokowa et al., 2012). There was also no effect on message levels for the LEF-1 transcriptional target C/EBPα, or on expression of CD11b, LY9, or PPARγ (Figure S3). Expression of Flt3 (a tyrosine kinase involved in myeloid progenitor cell differentiation that is frequently mutated in leukemia) was increased with FAS deficiency (Figure S3).

Using this abbreviated tamoxifen course, there was a striking decrease in peripheral blood white blood cells mostly due to fewer mature neutrophils (Figure 4A). There was also a striking loss of mature neutrophils in bone marrow (Figure 4B). Surprisingly, a modest increase in B cells (B220) and T cells (CD3) in the bone marrow was observed, suggesting a shift from myelopoiesis to lymphopoiesis. The same analyses performed in spleen showed a significant decrease in mature neutrophils (not shown).

To determine whether terminal granulocytic differentiation was altered in iFASKO mice, we assessed the frequency of granulocytic precursors in the bone marrow (Figure 4C). Granulocytic precursors can be classified based on the level of Gr-1 expression into early precursors (blasts and promyelocytes) and late precursors (myelocytes and metamyelocytes) (Hestdal et al., 1991). Despite the decrease in mature neutrophils, the number of early and late granulocytic precursors in iFASKO mice was comparable to control mice (Figure 4D).

We next asked whether the production of myeloid progenitors was altered in iFASKO mice. The number of myeloid progenitors and multipotent progenitors was assessed by flow cytometry (Figure 4E) as described (Akashi et al., 2000). The number of granulocyte-macrophage progenitors (GMPs) was similar to control mice (Figure 4F). Consistent with this observation, the number of colony forming unit-granulocyte/macrophage (CFU-GM) was similar in iFASKO and control mice (Figure 4I)). Interestingly, a significant increase in multipotent Kit^+ Sca^+ $lineage^-$ (KSL) cells and a trend to increased $CD150^+$ KSL cells, which are highly enriched for hematopoietic stem cells (Kiel et al., 2005), was observed in the bone marrow of iFASKO mice. Collectively, these results suggest that the loss of FAS specifically suppresses granulopoiesis, does not disrupt terminal granulocytic differentiation, and is associated with compensatory effects on myeloid progenitors.

Bone Marrow-specific FAS Deletion Produces Neutropenia without Lethality

We transplanted marrow from $FAS^{lox/lox}$/Rosa-Cre-ER+ or $FAS^{lox/lox}$/Rosa-Cre-ER- into lethally irradiated wild type C57 BL/6J mice (Figure 5A) and allowed the mice to recover for 5 weeks before treating them with tamoxifen. White blood cell counts were the same in mice 5 weeks after transplantation with floxed FAS with or without Rosa-Cre-ER (Figure 5B) and both groups of mice were phenotypically normal. On day 7 after tamoxifen treatment, white blood cells were significantly decreased in the mice that received marrow from $FAS^{lox/lox}$/Rosa-Cre-ER+ donors (Figure 5C), a decrement due to near complete loss of neutrophils. There was no effect on lymphocyte counts in the transplanted mice. These data suggest that loss of FAS in iFASKO mice produces a hematologic phenotype (Figure 3A) due to a cell autonomous loss of neutrophils but a non-cell autonomous loss of lymphocytes.

Despite neutropenia after tamoxifen treatment, bone marrow transplanted mice were viable (Figure 5D), indicating that death in iFASKO mice was due to the combination of intestinal barrier defects and neutropenia.

FAS Deficiency Causes Neutrophil Apoptosis and ER Stress

To address the mechanism underlying the cell autonomous neutrophil effect, we isolated marrow following the abbreviated tamoxifen course, removed red blood cells, and stained residual cells with a cocktail of antibodies to distinguish progenitor cells from differentiated cells. Cells that do not bind to these antibodies correspond to lineage-negative cells. Staining with annexin V-FITC to assess apoptosis followed by flow cytometry indicated that FAS deficiency caused cell death mainly in differentiated (mature) cells (Figure 6A).

Staining Gr-1 and Cd11b-positive bone marrow cells with annexin V-FITC and propidium iodide showed that apoptosis was increased in iFASKO neutrophils (Figure 6B), an observation confirmed by TUNEL staining (Figure 6C). Apoptosis is often associated with endoplasmic reticulum (ER) stress; the ER stress markers CHOP and Grp78 were increased in iFASKO neutrophils (Figure 6D). ER stress can be associated with alterations in membrane phospholipids, and lipidomic characterization of neutrophil membranes showed that numerous phosphatidylcholine (PC) species were decreased in iFASKO neutrophils (Figure 6E). Six of the 10 PC species that were decreased in iFASKO membranes were ether lipids, characterized by an ether bond instead of an ester bond at the sn-1 position. Phosphatidylethanolamine species were minimally affected (Figure 6F); total PC and PE mass values are shown in Figure 6G.

We also performed analyses to address the possibility that FAS deficiency affects other lipids in neutrophils. Plasmalogens were scarce, but one of the ether-linked phospholipids (16:0e/20:4-GPC, indicated by an arrow) shown in Figure 6E had a double bond adjacent to the ether bond at the sn-1 position indicative of a plasmalogen. This species was significantly decreased in iFASKO neutrophils. Platelet activating factor was not detected (not shown). Ceramides were also scarce, but the relative abundance of four ceramide species (d18:1/16:0, d18:1/24:2, d18:1/24:1, and d18:1/24:0) was significantly increased in iFASKO neutrophils compared to control neutrophils (Table S1), perhaps reflecting the induction of apoptosis occurring in these cells.

Lipidomic characterization of monocytes studied under the same conditions of induced FAS deficiency showed that while overall ether lipid abundance was low, several ether lipid species, all phosphatidylcholines, were significantly decreased (Table S2). Monocyte counts were not significantly decreased in iFASKO mice, but additional studies focused on monocyte biology would be required to determine if promotion of apoptosis associated with these lipid changes occurs only within the context of granulocytes.

Generation of Mice with Inducible Knockdown of PexRAP, the Terminal Enzyme in Ether Lipid Synthesis

Ether lipids are synthesized in peroxisomes (Lodhi and Semenkovich, 2014), and we recently identified PexRAP (Peroxisomal Reductase Activating PPAR) as the gene encoding the enzyme responsible for the terminal step in ether lipid synthesis (Lodhi et al., 2012).

Since ether lipids were decreased in iFASKO neutrophils during the process of cell loss, we generated a novel mouse model to test the hypothesis that the neutrophil phenotype was ether lipid dependent. We floxed the PexRAP locus in mice using the strategy depicted in Figure 7A with results of the PCR assay for genotyping heterozygous and homozygous floxed animals shown in Figure 7B. Floxed PexRAP mice were crossed with Rosa26-CreER mice to create PexRAP-iKO mice, and animals were treated with tamoxifen to induce Cre. Rearrangement at the PexRAP locus was confirmed (Figure 7C), and PexRAP expression was decreased in liver and bone marrow following tamoxifen (Figure 7D). Figure 7E shows representative spectra of phosphatidylcholine species from the bone marrow leukocytes of control and PexRAP-iKO mice with ether lipids labeled in red. Quantitation of these results (Figure 7F) demonstrated decreases in several ether lipid species as well as increases in acyl lipid species, perhaps reflecting compensation for ether lipid loss. Thus PexRAP inhibition is associated with decreased leukocyte ether lipid content, the expected biochemical consequences of this knockout.

Adult PexRAP-iKO mice were viable and had leukopenia due predominantly to the nearly complete loss of neutrophils (Figure 7G). There were also modest effects on lymphocytes, similar to iFASKO mice, and a small decrease in erythrocytes but not platelets (Figure S4).

Systemic activation of CreER alone using high doses of tamoxifen may cause hematologic toxicity characterized by severe anemia, a reduction in B cells, preferential effects on immature lineage cells, and no effect on myeloid cells (Higashi et al., 2009). Lower doses of tamoxifen (like those used in our experiments) are not associated with this effect (Higashi et al., 2009; Uhmann et al., 2009). In iFASKO mice, there was no anemia, an increase in B cell precursors, preferential effects on mature myeloid cells, and severe loss of myeloid cells, all different from effects of Cre alone. PexRAP-iKO mice (floxed at both PexRAP alleles) also showed severe loss of myeloid cells. We generated heterozygous foxed PexRAP mice in the presence or absence of CreER and treated all with tamoxifen. There was no significant difference in hematologic parameters for these mice (Table S3), suggesting that severe neutropenia in FAS knockout and PexRAP knockout animals is not due to Cre alone. There was a trend suggesting a gene dosage effect, consistent with a critical role for ether lipid synthesis in neutrophil biology.

When HL-60 cells, a cell line with neutrophil-like characteristics, were treated with a lentivirus to induce FAS knockdown, viability was compromised (Figure 7H, solid bar). Confirmation of the knockdown is shown in Figure 7I. When the FAS knockdown was performed in the presence of a mixture of 16:0 and 18:0 alkyl glycerol (a substrate for synthesis of ether-phosphatidylcholine species), this adverse effect on viability was partially rescued.

DISCUSSION

Our findings suggest that global deletion of FAS in adult mice causes death due to systemic endotoxemia in the setting of compromised intestinal barrier function and neutropenia. Neutropenia appears to result from increased ER stress and apoptosis caused by a preferential effect on the membrane content of peroxisome-derived ether lipids. A model

depicting this lipogenic pathway is shown in Figure 7J. These results establish an unrecognized link between endogenous lipid metabolism and inflammation, and provide proof of principle for inhibiting lipogenesis to selectively disrupt neutrophils.

Neutrophils defend against invading bacteria that have circumvented physical barriers provided by epithelial surfaces. Signaling molecules released by microorganisms activate blood vessel endothelial cells, which capture neutrophils and guide them into tissues (Borregaard, 2010). Factors produced by bacteria, such as the peptide N-formyl-methionine-leucinephenylalanine (fMLP), serve as chemotactic signals for recruitment of neutrophils, which defend the host through phagocytosis, release of bactericidal substances, and neutrophil extracellular traps, networks of DNA webs secreted by neutrophils that trap and kill invading bacteria (Borregaard, 2010).

FAS deficiency is associated with a marked and specific defect in granulopoiesis. The number of myeloid progenitors in the bone marrow of iFASKO mice is comparable to control mice, indicating the commitment to the myeloid lineage is not affected by FAS deficiency. Of note, the increase in multipotent progenitors (i.e., KSL cells) is likely secondary, in least in part, to the high systemic level of G-CSF (Schuettpelz et al., 2014). The normal number of granulocytic precursors in the bone marrow of iFASKO mice also indicates that FAS is dispensable for granulocytic differentiation. However, FAS is required for maintenance of mature neutrophils, and FAS deficiency is associated with increased neutrophil apoptosis. The bone marrow chimera studies show that this is mediated in a cell intrinsic fashion. These data raise the possibility that altered lipid metabolism renders FAS deficient neutrophils more susceptible to apoptosis. Consistent with this possibility, the neutrophil membrane composition is markedly altered in iFASKO mice. Specifically, peroxisome-derived ether-linked phospholipids are selectively decreased in FAS-deficient neutrophils. Of note, perturbation of cellular phospholipid composition influences membrane integrity (Li et al., 2006), activates ER stress (Fu et al., 2011; Volmer et al., 2013), and increases apoptosis (Yen et al., 1999).

FAS associates with peroxisomes, organelles important in lipid metabolism (Lodhi and Semenkovich, 2014). FAS is involved in generating ether-linked glycerophosphocholines that may be endogenous ligands for the nuclear receptor PPARγ in adipocytes, and FAS is enriched in adipocyte peroxisome fractions (Lodhi et al., 2012). FAS interacts with PMP70, a peroxisomal membrane protein involved in fatty acyl CoA transport into peroxisomes (Hillebrand et al., 2012), directly linking FAS to peroxisome lipid metabolism. Collectively, these results suggest that FAS channels fatty acids to peroxisomes for ether lipid synthesis.

Ether phospholipids carry an alkyl group attached to glycerol at the sn-1 position by an ether bond as opposed the ester bond present in conventional phospholipids. Ether lipid synthesis requires the dihydroxyacetone phosphate pathway (Hajra, 1995), the terminal step in this pathway is carried out at the peroxisomal membrane through a reductase activity purified four decades ago (LaBelle and Hajra, 1974), and we identified the gene encoding the protein responsible for this activity as PexRAP (Lodhi et al., 2012). In the current work, we show that tamoxifen-inducible knockout of PexRAP reduces ether-linked lipids and results in

neutrophil loss, phenocopying the results obtained with FAS deletion. Thus, it is likely that the FAS/PexRAP axis maintains membrane lipid composition and viability in neutrophils.

Ether lipids are scarce in most tissues, but curiously nearly half of the phosphatidylcholine pool in neutrophils is in the alkyl ether form (Brautigam et al., 1996; Mueller et al., 1984; Mueller et al., 1982). The role of ether lipids in this cell type is unclear but intracellular signaling is a possibility. Activation of neutrophils with fMLP increases diacylglycerol (DAG) as well as the ether lipid equivalent of DAG, 1-O-alkyl-2-acylglycerol (AAG). AAG production lags behind that of DAG (Dougherty et al., 1989). Since AAG inhibits DAG-mediated protein kinase C (PKC) activation (Bass et al., 1988), AAG induction may dampen the PKC-mediated respiratory burst in neutrophils. Ether lipids may also affect physical properties to regulate neutrophil function (Nagan and Zoeller, 2001).

Neutrophils are a vital component of innate immunity, but their hyperactivation or overproduction is detrimental. Reactive oxygen species and other mediators secreted by neutrophils kill pathogens but can also damage surrounding tissues. In rheumatoid arthritis, hyperactive neutrophils contribute to joint damage (Kaplan, 2013). In diet-induced obesity, neutrophils infiltrate tissues where their secretion of proteases promotes insulin resistance through degradation of insulin receptor substrate 1 (Talukdar et al., 2012). Treatment of human leukemia cells with an FAS inhibitor promotes apoptosis (Samudio et al., 2010), similar to the effects we observe in neutrophils with genetic inhibition of FAS or PexRAP. These findings suggest that targeted inhibition of lipogenic enzymes could alter the course of neutrophil-associated diseases.

EXPERIMENTAL PROCEDURES

Animals

To generate tamoxifen-inducible global FAS knockout (iFASKO) mice, floxed FAS ($FAS^{lox/lox}$) mice (Chakravarthy et al., 2005) were crossed with Rosa26-CreER mice (Badea et al. 2003) obtained from Jackson Laboratories. To induce Cre expression, iFASKO mice were treated with 50 μg/g body weight tamoxifen by intraperitoneal injection for five consecutive days as described (Remedi et al., 2009).

To generate mice with a floxed PexRAP allele (encoded by *dhrs7b*), a targeting vector for conditional knockout (design ID 39122) was obtained from the EUCOMM Repository. The targeting vector was generated by flanking a critical exon common to two known transcript variants of *dhrs7b* (i.e. exon 3 in the longer variant) with loxP sites such that following Cre-mediated deletion, a frameshift is created, resulting in nonsense-mediated decay of the message. The vector was linearized and electroporated into C57BL/6 embryonic stem (ES) cells. Out of 144 clones screened, 20 were properly targeted. One clone (C26) that had a normal karyotype was selected for micro-injection into B6(Cg)-Tyrc-2J/J blastocyts to generate chimeric mice. Highly chimeric mice were bred with B6(Cg)-Tyrc-2J/J females to select for germline transmission. To remove the neomycin selection cassette, the mice were first crossed with transgenic mice expressing Flp recombinase under the control of the actin promoter (Jackson Labs). The Flp transgene was removed by crossing the mice with wild-type C57 BL6/J mice. The mice were then crossed with Rosa26-CreER mice to generate

PexRAP-iKO mice. Rosa26-CreER was induced with tamoxifen as described above for iFASKO mice.

Genotyping of iFASKO was performed using previously described primer sets (Chakravathy et al. 2005). Floxed PexRAP mice were genotyped using primers P1 ($5'$GAA-CTG-TGT-GTG-TGT-ATC-TGC-CAG-T$3'$) and P2 ($5'$TCA-ACT-CTG-CTG-TAG-TGG-AGCAAG$3'$). To confirm Cre-mediated recombination in floxed PexRAP mice, primers P1 and P3 ($5'$CTT- CTG-GTG-TGT-CTG-AAG-ACA-ATG$3'$) were used. Diets included Purina 4043 control chow and Harlan Teklad TD 88137 high fat diet. Unless indicated otherwise, male iFASKO or PexRAP-iKO mice and respective control littermates at 8-12 weeks of age were used for experiments. The Washington University Animal Studies Committee approved animal protocols.

Complete Blood Counts

Peripheral blood from control and FAS or PexRAP knockout mice was collected into EDTA-coated tubes and analyzed in the Washington University Division of Comparative Medicine Research Animal Diagnostic Laboratory where automated complete and differential blood counts were performed. Trained technicians manually confirmed differential cell counts.

Flow Cytometry

Blood, bone marrow and spleen cells were harvested from mice using standard techniques, and the number of nucleated cells in these tissues was quantified using a Hemavet (Drew Scientific) or Cellometer Auto 2000 (Nexcelom) cell counter. Mononuclear cell preparations were lysed in Tris-Buffered ammonium chloride buffer, pH 7.2, and incubated with the indicated antibody at 4°C for 45 minutes in PBS containing 0.1% sodium azide, 1 mM EDTA, and 0.2% (wt/vol) bovine serum albumin to block non specific binding. For lineage analysis, the following directly conjugated monoclonal antibodies were used (all from eBioscience): APC-e780 Gr1 (RB6-8C5), APC B220 (RA3-6B2), PE CD115 (AFS98,), FITC CD11b (M1/70), PerCP-Cy5.5 CD3 (145-2C11). Hematopoietic progenitors were quantified as described (Akashi et al., 2000) using the following antibodies: PE-Cy7 CD3, B220, Gr-1, Terr119 (TER-119), APC e780 C-Kit (ACK2), APC Flt3 (A2F10), FITC CD34 (RAM34), PerCP-Cy5.5 Sca-1(D7), and BVe450 CD16/32 (93). All cells were analyzed using a FACScan flow cytometer (Becton Dickinson). Apoptosis assays used a mouse hematopoietic progenitor cell enrichment set consisting of biotin-conjugated monoclonal antibodies against CD3e, Cd11b, CD45R, Ly6G/Ly6C, and TER-119 from BD Pharmingen.

Apoptosis Assays

Apoptosis was measured by flow cytometry using the TACS Annexin V kit (Trevigen) as described by the manufacturer. FITC–Annexin V fluorescence was read with the FL1 photomultiplier tube and propidium iodide (PI) fluorescence was detected using the FL3 channel. Apoptosis was also assessed using the TUNEL Apoptosis Detection kit (Millipore) as described by the manufacturer.

CFU-C Assays

Bone marrow cells (5.0×10^4) were plated in 3 mL of methylcellulose media supplemented with a cocktail of recombinant cytokines (MethoCult 3434; StemCell Technologies). Cultures were plated in duplicate and placed in a humidified chamber with 5% CO_2 at 37°C. After 7 days of culture, the number of colonies per dish was counted.

Quantitative Real-time PCR

Total RNA was extracted using RNeasy Lipid Tissue kit (Qiagen) or the TRIzol reagent (Invitrogen) and reverse transcribed using iScript cDNA Synthesis kit (BioRad). Quantitative PCR was performed with an ABI Prism 7700 PCR instrument using SYBR® Green reagent (Applied Biosystems). Pre-validated primers spanning exon-exon boundaries were used for amplifications. Primer sequences are available upon request. Assays were performed in duplicate and results were normalized to ribosomal protein L32 mRNA levels, which were unaffected by genotype or intervention.

Analytical Procedures

Serum triglycerides, cholesterol, free fatty acids (FFA) and glucose were assayed in mice following a 4 h fast. Triglyceride and cholesterol levels were determined using reagents from Thermo Scientific. FFA levels were assayed using reagents provided by Wako Chemicals. Serum glucose was measured using reagents from Sigma. G-CSF was measured using a Quantikine ELISA from R&D Systems. Bacterial endotoxin was measured using a limulus amebocyte lysate assay (Wei et al. 2012). Body composition was determined using an EchoMRI 3-in-1 instrument (Echo Medical Systems). Western blotting was performed using a rabbit polyclonal anti-FAS antibody from Abcam, an anti-actin antibody from Sigma, and antibodies against CHOP and Grp78 from Cell Signaling.

Bone Marrow Transplantation

Bone marrow was harvested from the femurs and tibias of 12-week old non-tamoxifen-treated iFASKO or control (floxed but without Cre) mice by flushing bones with cold phosphate-buffered saline. Marrow was washed, triturated using a 24-gauge needle, collected by centrifugation at 1250 rpm for 4 min, and diluted with phosphate-buffered saline. After lysis of erythrocytes using 1X RBX Lysis Buffer (eBioscience), cells were counted to obtain a defined concentration of unfractionated bone marrow. Recipient wild type C57BL/6 mice were lethally irradiated with 10 gray from a cesium-137 γ-cell irradiator and infused with ~5×10^6 donor marrow cells within 6 h of irradiation. The fidelity of the process was confirmed by verifying the lethality of the radiation dose in animals not reconstituted with marrow, and by histological staining of recipient femurs. Six weeks after transplantation, the mice were treated with tamoxifen as described above. Complete blood count analysis was conducted prior to and after tamoxifen treatment.

Neutrophil Isolation

Mouse bone marrow was collected from femurs and tibias as described above. Following lysis of red blood cells, neutrophils were isolated by negative selection using the EasySep Mouse Neutrophil Enrichment kit (Stem Cell Technology) as described by the manufacturer.

Isolation of neutrophils was confirmed by positive staining for both Gr-1 and Cd11b using flow cytometry.

Cell Culture

HL-60 cells were maintained in Iscove's Modified Dulbecco's Medium (IMDM) supplemented with 20% FBS. HEK 293T cells were maintained in DMEM supplemented with 10% FBS.

Ether Lipid Supplementation in FAS Knockdown HL-60 Cells

Lentiviral FAS or scrambled shRNA was generated in 293T cells as previously described (Lodhi et al. 2012) and used to treat $5x10^6$ HL-60 cells together with a cocktail containing 5 μM each of 1-O-octadecyl-rac-glycerol (18:0-AG) and 1-O-hexadecyl-rac-glycerol (16:0-AG) or vehicle (ethanol). After 48 h, cells were treated with fresh media containing alkyl glycerol and puromycin. The cells were maintained under these conditions for an additional 72 h with media replaced every day. Cell viability was determined using the CellTiter96 assay (Promega) as described by the manufacturer.

Mass Spectrometry

Low-energy CAD tandem mass spectrometry was conducted on a Thermo Scientific (San Jose, CA) TSQ Vantage Triple Stage Quadrupole mass spectrometer equipped with Xcalibur operating system. Methanol/Chloroform (3/1, v/v, with 0.3% NH_4OH) was continuously infused into the ESI source with a syringe pump at a flow rate of 10 μL/min, and lipid extracts (with 14:0/14:0-PC and 14:0/14:0-PE internal standards added) dissolved in methanol/chloroform (3/1, v/v) were loop injected. The skimmer of the ESI source was at ground potential and the electrospray needle was set at 3.0 kV. The temperature of the heated capillary was 280° C. Q1 and Q3 quadrupole resolution was tuned to 0.7 Da (half width). The PC species in the total lipid extract was detected as $[M + H]^+$ ions by precursor ion scanning of m/z 184, while PE species were detected as $[M + H]^+$ ions by neutral loss scanning of 141 (Brugger et al., 1997). The collision energy was set at 30 eV and the Argon target gas was set at 1.0 mTorr. The tandem mass spectra were acquired by scanning from m/z 630 to m/z 850 at a rate of 2 s per scan. The mass spectra were acquired in profile mode and the final spectra represented the average of 40 spectra accumulated for 1 to 2 min.

Structural assignments of the glycerophospholipid species in lipid extracts were conducted on a Thermo Scientific (San Jose, CA) linear ion-trap (LIT) LTQ Orbitrap Velos mass spectrometer as described (Hsu et al., 2014).

Statistical Analysis

Comparisons between two groups were performed using an unpaired, two-tailed t test. ANOVA was used for more than two groups and post-testing was performed using Tukey's post test.

Supplementary Material

Refer to Web version on PubMed Central for supplementary material.

ACKNOWLEDGEMENTS

This work was supported by NIH grants DK076729, DK088083, DK20579, DK56341, K99 DK094874, and RR00954.

REFERENCES

Akashi K, Traver D, Miyamoto T, Weissman IL. A clonogenic common myeloid progenitor that gives rise to all myeloid lineages. Nature. 2000; 404:193–197. [PubMed: 10724173]

Badea TC, Wang Y, Nathans J. A noninvasive genetic/pharmacologic strategy for visualizing cell morphology and clonal relationships in the mouse. J Neurosci. 2003; 23:2314–2322. [PubMed: 12657690]

Bass DA, McPhail LC, Schmitt JD, Morris-Natschke S, McCall CE, Wykle RL. Selective priming of rate and duration of the respiratory burst of neutrophils by 1,2-diacyl and 1-O-alkyl-2-acyl diglycerides. Possible relation to effects on protein kinase C. J Biol Chem. 1988; 263:19610–19617. [PubMed: 3198643]

Bernal-Mizrachi C, Weng S, Feng C, Finck BN, Knutsen RH, Leone TC, Coleman T, Mecham RP, Kelly DP, Semenkovich CF. Dexamethasone induction of hypertension and diabetes is PPAR-alpha dependent in LDL receptor-null mice. Nat Med. 2003; 9:1069–1075. [PubMed: 12847522]

Borregaard N. Neutrophils, from marrow to microbes. Immunity. 2010; 33:657–670. [PubMed: 21094463]

Brautigam C, Engelmann B, Reiss D, Reinhardt U, Thiery J, Richter WO, Brosche T. Plasmalogen phospholipids in plasma lipoproteins of normolipidemic donors and patients with hypercholesterolemia treated by LDL apheresis. Atherosclerosis. 1996; 119:77–88. [PubMed: 8929259]

Brugger B, Erben G, Sandhoff R, Wieland FT, Lehmann WD. Quantitative analysis of biological membrane lipids at the low picomole level by nano-electrospray ionization tandem mass spectrometry. Proc Natl Acad Sci USA. 1997; 94:2339–2344. [PubMed: 9122196]

Chakravarthy MV, Lodhi IJ, Yin L, Malapaka RR, Xu HE, Turk J, Semenkovich CF. Identification of a physiologically relevant endogenous ligand for PPARalpha in liver. Cell. 2009; 138:476–488. [PubMed: 19646743]

Chakravarthy MV, Pan Z, Zhu Y, Tordjman K, Schneider JG, Coleman T, Turk J, Semenkovich CF. "New" hepatic fat activates PPARalpha to maintain glucose, lipid, and cholesterol homeostasis. Cell Metab. 2005; 1:309–322. [PubMed: 16054078]

Chakravarthy MV, Zhu Y, Lopez M, Yin L, Wozniak DF, Coleman T, Hu Z, Wolfgang M, Vidal-Puig A, Lane MD, et al. Brain fatty acid synthase activates PPARalpha to maintain energy homeostasis. J Clin Invest. 2007; 117:2539–2552. [PubMed: 17694178]

Chirala SS, Chang H, Matzuk M, Abu-Elheiga L, Mao J, Mahon K, Finegold M, Wakil SJ. Fatty acid synthesis is essential in embryonic development: fatty acid synthase null mutants and most of the heterozygotes die in utero. Proc Natl Acad Sci USA. 2003; 100:6358–6363. [PubMed: 12738878]

Day RB, Link DC. Regulation of neutrophil trafficking from the bone marrow. Cell Mol Life Sci. 2012; 69:1415–1423. [PubMed: 22045556]

Dougherty RW, Dubay GR, Niedel JE. Dynamics of the diradylglycerol responses of stimulated phagocytes. J Biol Chem. 1989; 264:11263–11269. [PubMed: 2500437]

Fu S, Yang L, Li P, Hofmann O, Dicker L, Hide W, Lin X, Watkins SM, Ivanov AR, Hotamisligil GS. Aberrant lipid metabolism disrupts calcium homeostasis causing liver endoplasmic reticulum stress in obesity. Nature. 2011; 473:528–531. [PubMed: 21532591]

Funai K, Song H, Yin L, Lodhi IJ, Wei X, Yoshino J, Coleman T, Semenkovich CF. Muscle lipogenesis balances insulin sensitivity and strength through calcium signaling. J Clin Invest. 2013; 123:1229–1240. [PubMed: 23376793]

Hajra AK. Glycerolipid biosynthesis in peroxisomes (microbodies). Prog Lipid Res. 1995; 34:343–364. [PubMed: 8685243]

Hestdal K, Ruscetti FW, Ihle JN, Jacobsen SE, Dubois CM, Kopp WC, Longo DL, Keller JR. Characterization and regulation of RB6-8C5 antigen expression on murine bone marrow cells. J Immunol. 1991; 147:22–28. [PubMed: 1711076]

Higashi AY, Ikawa T, Muramatsu M, Economides AN, Niwa A, Okuda T, Murphy AJ, Rojas J, Heike T, Nakahata T, Kawamoto H, Kita T, Yanagita M. Direct hematological toxicity and illegitimate chromosomal recombination caused by the systemic activation of CreER^{T2}. J Immunol. 2009; 182:5633–5640. [PubMed: 19380810]

Hillebrand M, Gersting SW, Lotz-Havla AS, Schafer A, Rosewich H, Valerius O, Muntau AC, Gartner J. Identification of a new fatty acid synthesis-transport machinery at the peroxisomal membrane. J Biol Chem. 2012; 287:210–221. [PubMed: 22045812]

Hooper LV. Do symbiotic bacteria subvert host immunity? Nat Rev Microbiol. 2009; 7:367–374. [PubMed: 19369952]

Hsu FF, Lodhi IJ, Turk J, Semenkovich CF. Structural Distinction of Diacyl-, Alkylacyl, and Alk-1-Enylacyl Glycerophosphocholines as [M -15] Ions by Multiple-Stage Linear Ion-Trap Mass Spectrometry with Electrospray Ionization. J Am Soc Mass Spectrom. Apr 30.2014 Epub ahead of print.

Jensen-Urstad AP, Semenkovich CF. Fatty acid synthase and liver triglyceride metabolism: housekeeper or messenger? Biochim Biophys Acta. 2012; 1821:747–753. [PubMed: 22009142]

Jensen-Urstad AP, Song H, Lodhi IJ, Funai K, Yin L, Coleman T, Semenkovich CF. Nutrient-dependent phosphorylation channels lipid synthesis to regulate PPARalpha. J Lipid Res. 2013; 54:1848–1859. [PubMed: 23585690]

Johansson ME, Thomsson KA, Hansson GC. Proteomic analyses of the two mucus layers of the colon barrier reveal that their main component, the Muc2 mucin, is strongly bound to the Fcgbp protein. J Proteome Res. 2009; 8:3549–3557. [PubMed: 19432394]

Kaplan MJ. Role of neutrophils in systemic autoimmune diseases. Arth Res Ther. 2013; 15:219. [PubMed: 24286137]

Kiel MJ, Yilmaz OH, Iwashita T, Terhorst C, Morrison SJ. SLAM family receptors distinguish hematopoietic stem and progenitor cells and reveal endothelial niches for stem cells. Cell. 2005; 121:1109–1121. [PubMed: 15989959]

Knobloch M, Braun SM, Zurkirchen L, von Schoultz C, Zamboni N, Arauzo-Bravo MJ, Kovacs WJ, Karalay O, Suter U, Machado RA, et al. Metabolic control of adult neural stem cell activity by Fasn-dependent lipogenesis. Nature. 2013; 493:226–230. [PubMed: 23201681]

LaBelle EF Jr. Hajra AK. Purification and kinetic properties of acyl and alkyl dihydroxyacetone phosphate oxidoreductase. J Biol Chem. 1974; 249:6936–6944. [PubMed: 4153765]

Li Z, Agellon LB, Allen TM, Umeda M, Jewell L, Mason A, Vance DE. The ratio of phosphatidylcholine to phosphatidylethanolamine influences membrane integrity and steatohepatitis. Cell Metab. 2006; 3:321–331. [PubMed: 16679290]

Liu F, Wu HY, Wesselschmidt R, Kornaga T, Link DC. Impaired production and increased apoptosis of neutrophils in granulocyte colony-stimulating factor receptor-deficient mice. Immunity. 1996; 5:491–501. [PubMed: 8934575]

Lodhi IJ, Semenkovich CF. Peroxisomes: a nexus for lipid metabolism and cellular signaling. Cell Metab. 2014; 19:380–392. [PubMed: 24508507]

Lodhi IJ, Yin L, Jensen-Urstad AP, Funai K, Coleman T, Baird JH, El Ramahi MK, Razani B, Song H, Fu-Hsu F, et al. Inhibiting adipose tissue lipogenesis reprograms thermogenesis and PPARgamma activation to decrease diet-induced obesity. Cell Metab. 2012; 16:189–201. [PubMed: 22863804]

Menendez JA, Lupu R. Fatty acid synthase and the lipogenic phenotype in cancer pathogenesis. Nat Rev Cancer. 2007; 7:763–777. [PubMed: 17882277]

Moreno-Navarrete JM, Botas P, Valdes S, Ortega FJ, Delgado E, Vazquez-Martin A, Bassols J, Pardo G, Ricart W, Menendez JA, et al. Val1483Ile in FASN gene is linked to central obesity and insulin sensitivity in adult white men. Obesity (Silver Spring). 2009; 17:1755–1761. [PubMed: 19300427]

Mueller HW, O'Flaherty JT, Greene DG, Samuel MP, Wykle RL. 1-O-alkyl-linked glycerophospholipids of human neutrophils: distribution of arachidonate and other acyl residues in the ether-linked and diacyl species. J Lipid Res. 1984; 25:383–388. [PubMed: 6427378]

Mueller HW, O'Flaherty JT, Wykle RL. Ether lipid content and fatty acid distribution in rabbit polymorphonuclear neutrophil phospholipids. Lipids. 1982; 17:72–77. [PubMed: 7087685]

Nagan N, Zoeller RA. Plasmalogens: biosynthesis and functions. Prog Lipid Res. 2001; 40:199–229. [PubMed: 11275267]

Razani B, Zhang H, Schulze PC, Schilling JD, Verbsky J, Lodhi IJ, Topkara VK, Feng C, Coleman T, Kovacs A, et al. Fatty acid synthase modulates homeostatic responses to myocardial stress. J Biol Chem. 2011; 286:30949–30961. [PubMed: 21757749]

Reddy JK, Hashimoto T. Peroxisomal beta-oxidation and peroxisome proliferator-activated receptor alpha: an adaptive metabolic system. Annu Rev Nutr. 2001; 21:193–230. [PubMed: 11375435]

Remedi MS, Kurata HT, Scott A, Wunderlich FT, Rother E, Kleinridders A, Tong A, Bruning JC, Koster JC, Nichols CG. Secondary consequences of beta cell inexcitability: identification and prevention in a murine model of K(ATP)-induced neonatal diabetes mellitus. Cell Metab. 2009; 9:140–151. [PubMed: 19187772]

Roberts R, Hodson L, Dennis AL, Neville MJ, Humphreys SM, Harnden KE, Micklem KJ, Frayn KN. Markers of de novo lipogenesis in adipose tissue: associations with small adipocytes and insulin sensitivity in humans. Diabetologia. 2009; 52:882–890. [PubMed: 19252892]

Samudio I, Harmancey R, Fiegl M, Kantarjian H, Konopleva M, Korchin B, Kaluarachchi K, Bornmann W, Duvvuri S, Taegtmeyer H, et al. Pharmacologic inhibition of fatty acid oxidation sensitizes human leukemia cells to apoptosis induction. J Clin Invest. 2010; 120:142–156. [PubMed: 20038799]

Schneider JG, Yang Z, Chakravarthy MV, Lodhi IJ, Wei X, Turk J, Semenkovich CF. Macrophage fatty-acid synthase deficiency decreases diet-induced atherosclerosis. J Biol Chem. 2010; 285:23398–23409. [PubMed: 20479009]

Schuettpelz LG, Borgerding JN, Christopher MJ, Gopalan PK, Romine MP, Herman AC, Woloszynek JR, Greenbaum AM, Link DC. G-CSF regulates hematopoietic stem cell activity, in part, through activation of Toll-like receptor signaling. Leukemia. Feb 12.2014 Epub ahead of print.

Skokowa J, Cario G, Uenalan M, Schambach A, Germeshausen M, Battmer K, Zeidler C, Lehmann U, Eder M, Baum C, et al. LEF-1 is crucial for neutrophil granulocytopoiesis and its expression is severely reduced in congenital neutropenia. Nat Med. 2006; 12:1191–1197. [PubMed: 17063141]

Skokowa J, Klimiankou M, Klimenkova O, Lan D, Gupta K, Hussein K, Carrizosa E, Kusnetsova I, Li Z, Sustmann C, et al. Interactions among HCLS1, HAX1 and LEF-1 proteins are essential for G-CSF-triggered granulopoiesis. Nat Med. 2012; 18:1550–1559. [PubMed: 23001182]

Talukdar S, Oh da Y, Bandyopadhyay G, Li D, Xu J, McNelis J, Lu M, Li P, Yan Q, Zhu Y, et al. Neutrophils mediate insulin resistance in mice fed a high-fat diet through secreted elastase. Nat Med. 2012; 18:1407–1412. [PubMed: 22863787]

Uhmann A, Dittmann K, Wienand J, Hahn H. Comment on “Direct hematological toxicity and illegitimate chromosomal recombination caused by the systemic activation of CreER^{T2}”. J Immunol. 2009; 183:2891. [PubMed: 19696426]

Volmer R, van der Ploeg K, Ron D. Membrane lipid saturation activates endoplasmic reticulum unfolded protein response transducers through their transmembrane domains. Proc Natl Acad Sci USA. 2013; 110:4628–4633. [PubMed: 23487760]

Wei X, Schneider JG, Shenouda SM, Lee A, Towler DA, Chakravarthy MV, Vita JA, Semenkovich CF. De novo lipogenesis maintains vascular homeostasis through endothelial nitric-oxide synthase (eNOS) palmitoylation. J Biol Chem. 2011; 286:2933–2945. [PubMed: 21098489]

Wei X, Yang Z, Rey FE, Ridaura VK, Davidson NO, Gordon JI, Semenkovich CF. Fatty acid synthase modulates intestinal barrier function through palmitoylation of mucin 2. Cell Host Microbe. 2012; 11:140–152. [PubMed: 22341463]

Yen CL, Mar MH, Zeisel SH. Choline deficiency-induced apoptosis in PC12 cells is associated with diminished membrane phosphatidylcholine and sphingomyelin, accumulation of ceramide and diacylglycerol, and activation of a caspase. FASEB J. 1999; 13:135–142. [PubMed: 9872938]

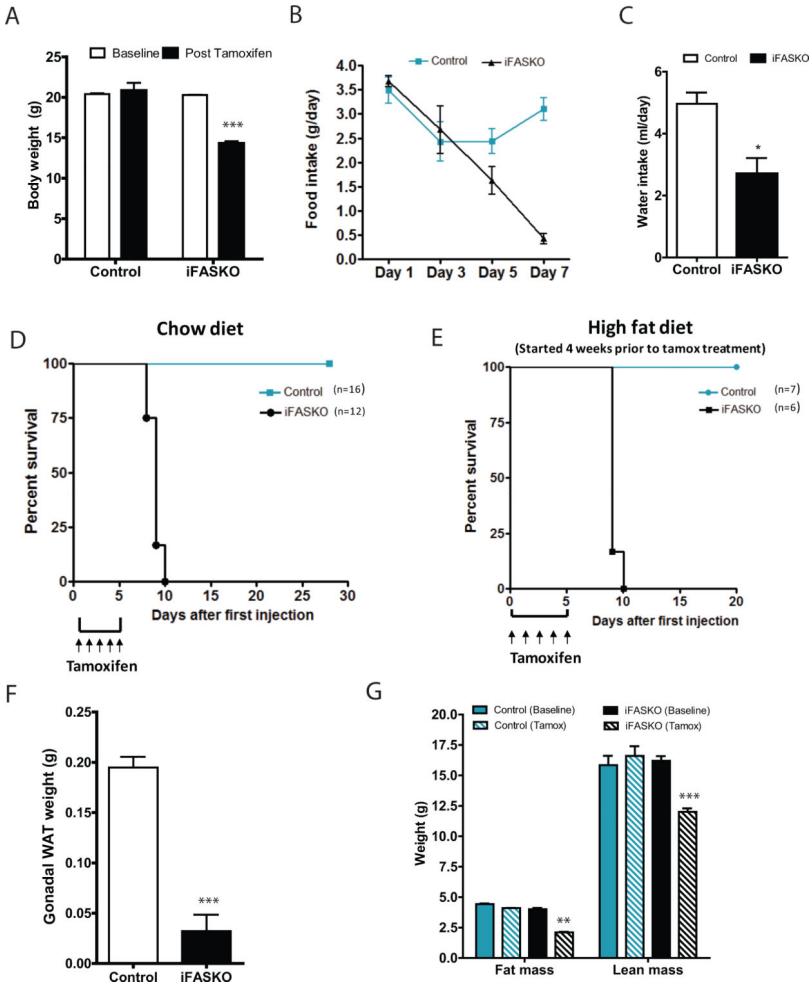

Figure 1. Tamoxifen-inducible FAS knockout in adult mice is lethal

(A) Body weight of control and iFASKO mice before and after tamoxifen treatment.

(B) Food intake. Data are from 5 animals per genotype.

(C) Water intake on day 5 after tamoxifen treatment.

(D and E) Kaplan-Meier survival curves of control and iFASKO fed chow or high fat diet.

(F) Weight of gonadal white adipose tissue (WAT) in control and iFASKO mice treated with tamoxifen.

(G) MRI analysis of body composition of control and iFASKO mice before and after tamoxifen treatment.

In all panels, the mice were treated with tamoxifen for five days and analyzed on day 7 after the initial treatment, unless otherwise indicated. Data are expressed as mean ± SEM of at least 5 animals per genotype. *P<0.05. **P<0.01. ***P<0.001.

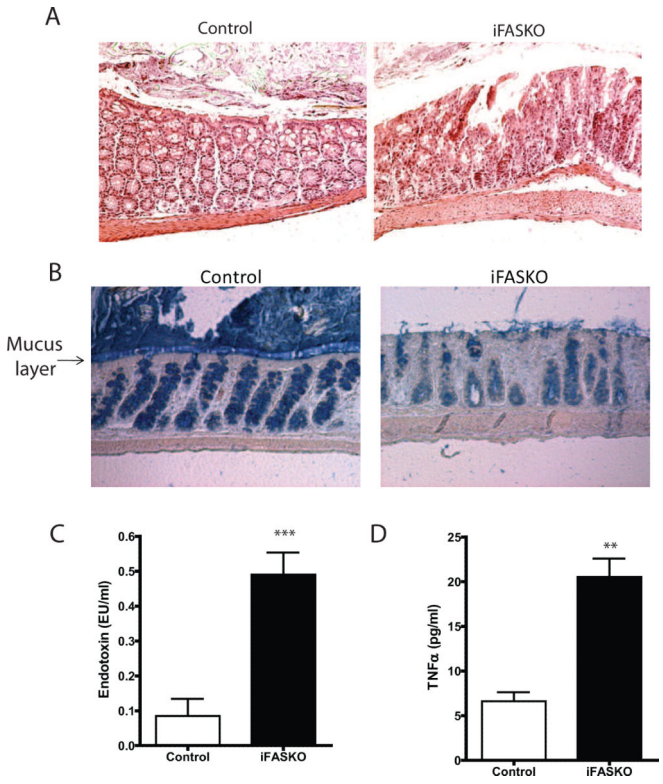

Figure 2. Tamoxifen-inducible FAS knockout mice have a compromised intestinal barrier

(A) H&E staining of colon from control and iFASKO mice.

(B) Alcian blue staining of goblet cells of the large intestine in control and iFASKO mice.

(C) Serum endotoxin levels. Data are expressed as mean ± SEM of 6-7 animals per genotype. ***P<0.001.

(D) Serum TNFα levels. **P<0.01.

In all panels, the mice were treated with tamoxifen for five days and analyzed on day 7 after the initial treatment. Data are expressed as mean ± SEM of 3-5 animals per genotype.

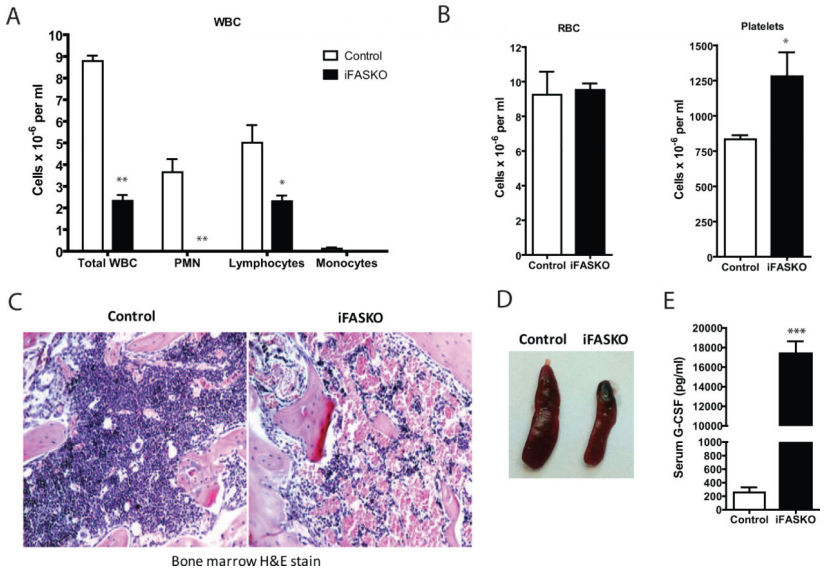

Figure 3. FAS knockout in adult mice causes a defect in hematopoiesis

In all panels, the mice were treated with tamoxifen for five days and analyzed on day 7 after the initial treatment.

(A and B) Blood count analysis of peripheral blood from control and iFASKO mice. Data are expressed as mean ± SEM of 4 animals per genotype. *P<0.05. **P<0.01.

(C) H&E staining of bone marrow of control and iFASKO mice.

(D) Spleen from control and iFASKO mice.

(E) Serum G-CSF determination. Data are expressed as mean ± SEM of 5 animals per genotype. ***P<0.0001.

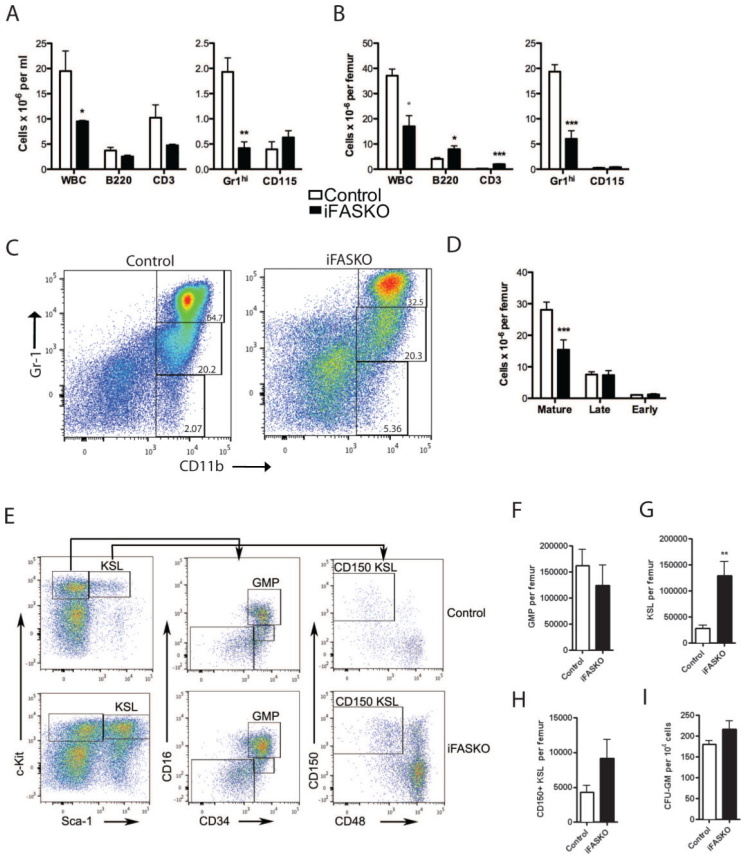

Figure 4. Loss of FAS impairs granulopoiesis but does not disrupt terminal differentiation or production of myeloid progenitors

In all panels, the mice were treated with tamoxifen for three days and analyzed on day 4.

(A and B) Blood count analysis of peripheral blood (A) and bone marrow (B). The number of white blood cells, (WBC), B cells (B220), T cells (CD3), neutrophils ($Gr1^{hi}$), and monocytes (CD115) is shown. Data are expressed as mean ± SEM of 4 animals per genotype. *P<0.05. **P<0.01.

(C) Representative dot plots showing Gr-1 and CD11b staining of bone marrow cells; data are gated on $B220^{-}$, $CD3^{-}$, and $CD115^{-}$ cells. Mature neutrophils (top gate) are identified as $Gr1^{hi}$ cells, late granulocytic precursors as $Gr1^{Int}$ cells (middle gate), and early granulocytic precursors as $Gr1^{low}$ cells (lower gate).

(D) Number of mature neutrophils or granulocytic precursors in the bone marrow. Data are expressed as mean ± SEM of 4-5 mice. ***P<0.001.

(E) Representative dot plots showing the gating strategy to identify granulocyte-macrophage progenitors (GMPs), Kit^{+} Sca^{+} $lineage^{-}$ (KSL) cells, or $CD150^{+}$ KSL cells.

(F-I) Progenitor analysis. Data are expressed as mean ± SEM of 4-5 mice. **P<0.01.

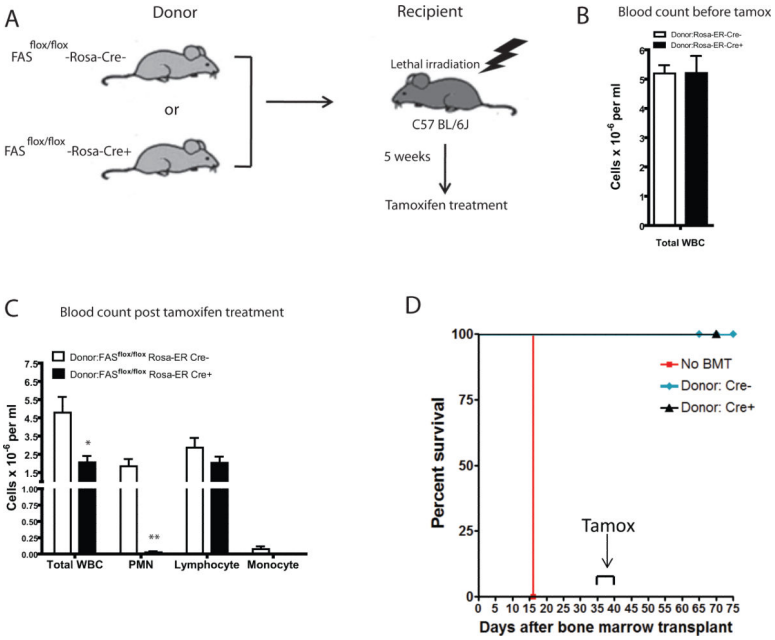

Figure 5. Bone marrow-restricted FAS knockout causes neutropenia, but not lethality

(A) Schematic diagram of bone marrow transplant experiment. The recipient mice were allowed to recover for 5 weeks and then treated with tamoxifen for 5 days.

(B) Total white blood cell count in mice that received marrow from Cre – or Cre+ donor mice prior to tamoxifen treatment.

(C) Total and differential white blood cell count in bone marrow transplant mice after tamoxifen treatment. Data are expressed as mean ± SEM of 5 animals per genotype. *P<0.05. **P<0.01.

(D) Kaplan-Meier survival curve of bone marrow transplant mice.

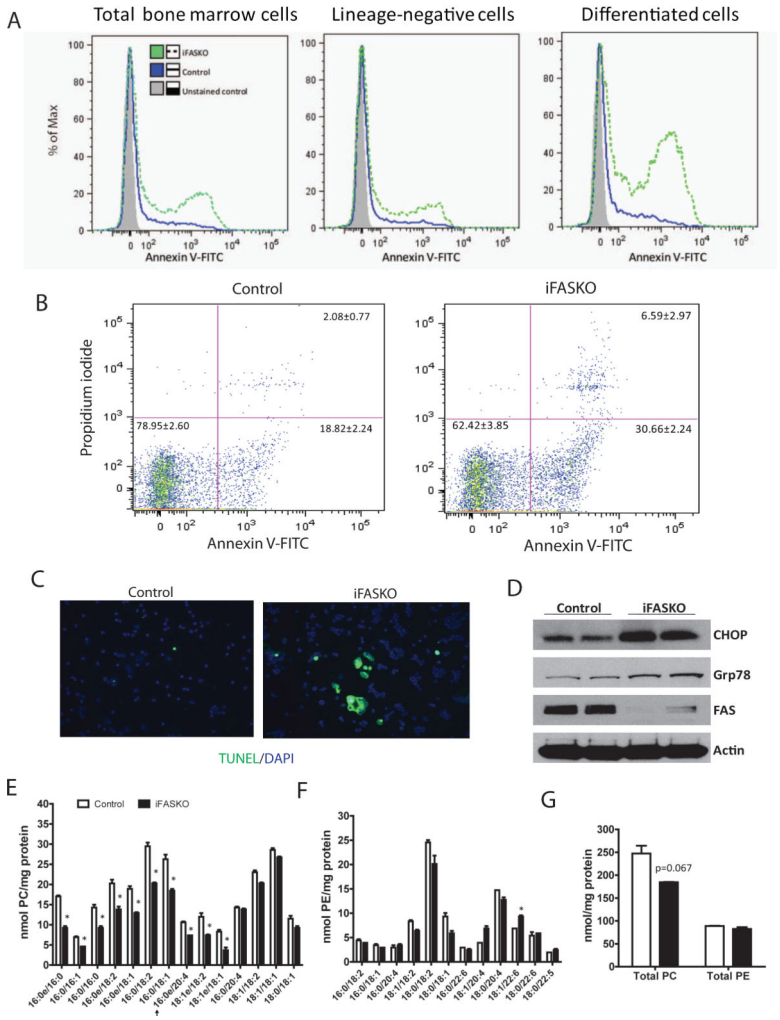

Figure 6. FAS knockout causes neutrophil apoptosis, ER stress and preferentially decreases membrane ether-linked glycerophosphocholines

Control and iFASKO mice were treated with tamoxifen for three days and bone marrow was harvested on day 4.

(A) Following removal of red blood cells, the remaining cells were stained with a cocktail of antibodies that recognize differentiated cells in the marrow, and then stained with annexin V and analyzed by FACSCAN.

(B) Cells were stained with neutrophil makers Gr-1 and Cd11b, and then stained with annexin V and propidium and analyzed by FACSCAN. Data represent 5-6 mice per genotype. *P<0.05.

(C) TUNEL staining of neutrophils from control and iFASKO mice.

(D) Western blot analysis of neutrophils from control and iFASKO mice.

(E-G) Determination of membrane phospholipids. Control and iFASKO mice were treated with tamoxifen for three days and bone marrow was harvested on day 4. Following removal of red blood cells, the neutrophils were harvested by negative selection. Phospholipid composition was analyzed by mass spectrometry. Ether-linked phospholipids are denoted by “e” and the single plasmalogen identified is indicated by the arrow in panel E. Data are

mean ± SD of duplicate determinations using pooled extracts from 4 mice per genotype. *P<0.05.

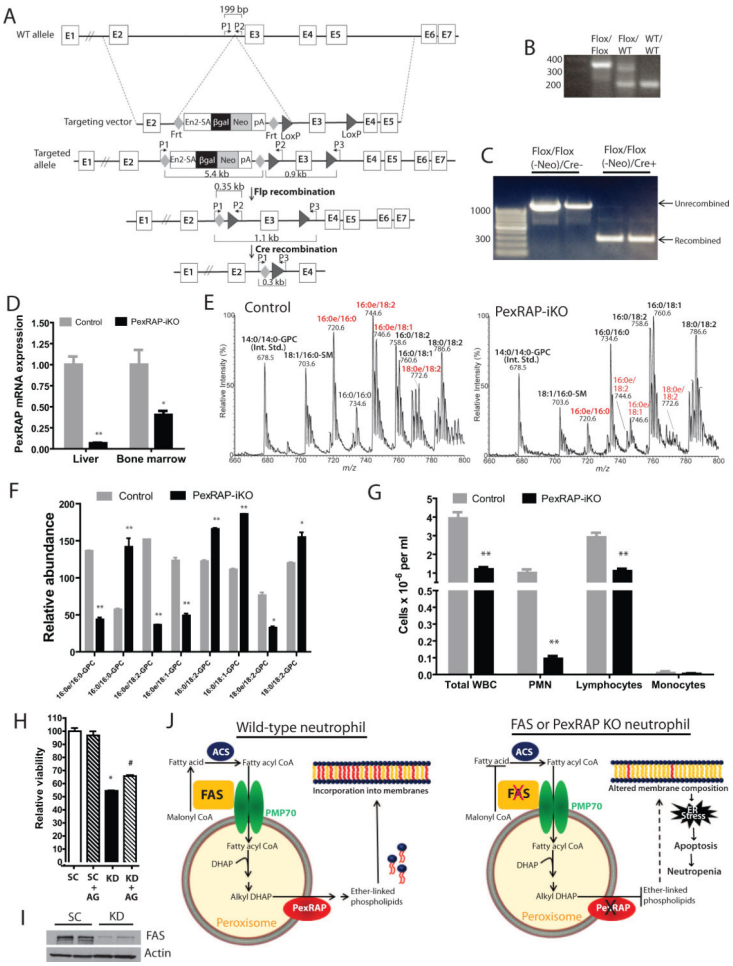

Figure 7. Tamoxifen-inducible knockout of the ether lipid synthetic enzyme PexRAP causes neutropenia and ether lipid supplementation in HL-60 cells partially rescues cell loss

(A) Targeting strategy for generation of PexRAP conditional knockout mice.

(B) Genotyping of PexRAP homozygous floxed, heterozygous floxed, and wild type mice by PCR using primers P1 and P2 and tail DNA.

(C) Confirmation of Cre-mediated recombination by PCR using primers P1 and P3 in livers of mice treated with tamoxifen.

(D) Real-time PCR analysis of mRNA expression in liver and bone marrow of mice on day 5 after 4 consecutive daily treatments with tamoxifen. Data are expressed as mean ± SEM of 3 mice per genotype. *P<0.05. **P<0.001.

(E) Representative mass spectra of GPCs from bone marrow white blood cells of control and PexRAP-iKO mice. The mice were treated with tamoxifen as described in panel (D). Ether-linked GPCs are indicated in red.

(F) Quantification of relative abundance of GPCs. Data represent mean ± SD of duplicate determinations in 3 mice per genotype. *P<0.05; **P<0.001.

(G) Peripheral blood count analysis of control and PexRAP-iKO mice. The mice were treated with tamoxifen for 5 consecutive days and the blood was collected on day 7. Data are mean ± SEM of 4 animals per genotype. **P<0.001.

(H) Effect of alkyl glycerol (AG) supplementation viability of HL-60 cells treated with scrambled (control) or FAS shRNA. Data are mean ±SEM of 3 separate determinations. *P<0.05 vs. SC; #p<0.05 vs. KD.

(I) Western blot of FAS knockdown in HL-60 cells.

(J) Proposed model of the role of lipogenesis in maintaining viability and membrane integrity in neutrophils. ACS is acyl-CoA synthetase, DHAP is dihydroxyacetone phosphate, PMP70 is peroxisomal membrane protein of 70 kD.